



Influence of the polymer structure of polycarboxylate-based superplasticizers on the intercalation behaviour in montmorillonite clays

Pere Borralleras^a, Ignacio Segura^{b,c,*}, Miguel A.G. Aranda^d, Antonio Aguado^b

^a BASF Construction Chemicals Iberia, Ctra del Mig 219, E-08907 Hospitalet de Llobregat, Barcelona, Spain

^b Department of Environmental and Civil Engineering, Universitat Politècnica de Catalunya-Barcelona Tech, Jordi Girona 1-3, C1, E-08034 Barcelona, Spain

^c Smart Engineering Ltd, Jordi Girona 1-3, ParcUPC – K2M, E-08034 Barcelona, Spain

^d ALBA Synchrotron, Carrer de la Llum 2-26, E-08290, Cerdanyola del Vallès, Barcelona, Spain

HIGHLIGHTS

- In-situ XRD reveals how the PCE structure influences in the intercalation process.
- Clay expansion profiles are aligned with fluidity and sorption behavior.
- PCE with long side chain and high grafting ratio produce larger expansion of clay; high side chain density promote clay exfoliation at lower dosage.
- PCE with high anionic charge needs lower dosage to saturate the interlaminar space.
- Exfoliation of clay enhances the interference on PCE performance.

ARTICLE INFO

Article history:

Received 13 December 2018

Received in revised form 27 May 2019

Accepted 3 June 2019

Available online 10 June 2019

Keywords:

XRD (C)

Polycarboxylate (E)

Clay (C)

d-spacing (E)

Synchrotron radiation (C)

Intercalation (D)

Exfoliation (C)

ABSTRACT

The influence of polymeric structure of polycarboxylate-ether (PCE) based superplasticizers on the intercalation behavior in sodium montmorillonite clay (Na-MNT) is investigated by performing *in-situ* X-ray diffraction (XRPD) on fresh, unaltered clay pastes. The use of this technique reveals the real influence of the PCE structure and of the PCE/clay dosage ratio on the expansion profile of the clay. This is not observed with the traditional XRPD methodology performed on dried clay pastes, which shows the same values of d-spacing despite using polymers of diverse structures. It is observed that PCE polymers with long side chains and high side chain density result in larger expansion. Additionally, polymers with a high anionic charge saturate the interlaminar space of montmorillonite at a lower dosage. The experimental results also indicate that clay exfoliation is critical in the intercalation process and the exfoliation tendency of the clay is influenced by the structure of PCE polymers.

© 2019 Elsevier Ltd. All rights reserved.

1. Introduction

The dispersing capacity and water reduction efficiency of polycarboxylate-ether (PCE) based superplasticizers is severally affected by the presence of montmorillonite clays (MNT) in the sands used for concrete production. This type of clays has the ability to absorb large quantities of PCE polymers through an intercalation mechanism of the PEG/PEO (poly-ethylene glycol/poly-

ethylene oxide) side chains of the polymer [1,2], which is responsible for the partial or total loss of their dispersing capacity.

The absorption behaviour of PCE-based superplasticizers on MNT clay has already been investigated by different authors using XRPD analysis on centrifuged and dried clay pastes [1,2]. These studies show almost no influence on the d-spacing of MNT clay when different structures of PCE polymers are used since the maximum clay expansion value always remains in the range of 18–21 Å and, in all cases, the average differences of d_{001} values within PCE polymers of diverse structures does not exceed 3 Å (the distance equivalent to one water molecule arranged in the interlayer of MNT clays).

The intercalation level associated with the d-spacing measured by traditional XRPD on dried pastes corresponds to one monolayer

* Corresponding author at: Department of Environmental and Civil Engineering, Universitat Politècnica de Catalunya-Barcelona Tech, Jordi Girona 1-3, C1, E-08034 Barcelona, Spain.

E-mail address: ignacio.segura@upc.edu (I. Segura).

of PEG/PEO (poly-ethylene glycol/poly-ethylene oxide) side chains intercalated into the interlaminar space of MNT clay with two coordination water molecules [2–5]. Since the net expansion of 3 Å is equivalent to a one single water molecule layer or to a one single monolayer of PEG/PEO side chain intercalated into the interlaminar space of MNT clay [6], it indicates that the same intercalation degree of side chains is inferred by applying the traditional analytical technique. Thus, this methodology does not allow to determine whether the structure of the PCE polymers has influence in the expansion behaviour of MNT clay that induced by the intercalation of side chains.

Therefore, by relying on the experimental results from XRPD analysis performed on centrifuged and dried clay pastes, it should be concluded that there is almost no influence of the structure of PCE polymers in the intercalation degree of side chains. Nevertheless, fluidity tests for cement pastes containing MNT clay and PCE based superplasticizers shows significant differences in the paste flow loss for different PCE structures [2,7,8]. These experimental results confirm that the structure of PCE polymer has a more relevant role in the interaction process with the clay versus the conclusions deduced from the XRPD analysis on centrifuged and dried clay pastes.

The objective of this study is to identify the influence of the polymer structure of PCE-based superplasticizers in the interaction process with MNT clays by performing *in situ* XRPD analysis on fresh, unaltered clay pastes. The authors previously demonstrated the methodology for *in-situ* XRPD characterization and the information that can be obtained for MNT clay expansion [6]. This allows researchers to identify increased intercalation degrees than those previously deduced by the traditional analytic methodology. It also demonstrates greater influence of PCE dosage on the dispacing evolution.

2. Research significance

As far as the authors know, this is the first study using *in-situ* XRPD measurements on fresh, unaltered clay pastes to examine the intercalation mechanism of PCE-based superplasticizers in montmorillonite clays and the influence of the polymer structure in this process. Several investigations have previously studied this process using traditional XRPD analysis on centrifuged and dried clay pastes [1–5]. However, the conclusions extracted from the experimental results did not offer a clear view on the influence of the PCE structure in the intercalation mechanism.

Table 1
Oxide composition and mineral phases of anhydrous cement used.

Oxide composition (wt%)		Mineral phases (wt%)	
SiO ₂	19.60	C ₃ S	58.9
Al ₂ O ₃	5.38	C ₂ S	14.0
Fe ₂ O ₃	2.41	C ₃ A total	9.4
CaO	65.29	C ₃ A ort/cub	99% cubic
Na ₂ O	0.05	C ₄ (A,F)	5.7
K ₂ O	0.84	M _x (SO ₄)	5.5
MgO	0.82	Total	93.5
SO ₃	3.34		
LOI	2.18		

Table 2
Oxide composition of MNT clay used.

Oxide composition of Na-MNT (wt%)										
SiO ₂	TiO ₂	Al ₂ O ₃	Fe ₂ O ₃	MgO	MnO	NiO	CaO	K ₂ O	Na ₂ O	LOI
63.12	0.01	19.88	1.37	2.33	0.04	0.06	2.24	0.44	3.43	5.97

3. Materials

3.1. Cement

Cement pastes are prepared with cement type CEM I 52.5R. Table 1 presents oxide and mineral phase composition of anhydrous cement (expressed in wt. %) determined by XRF (X-ray fluorescence). The Blaine value reported in cement specifications is 4750 cm²/g. The measured BET-specific surface is 1.6 m²/g and the particle size (D₅₀), determined by laser diffraction, is 10 μm. For the reproducibility of the experimental results obtained in this study, it should be stated that the amount of orthorhombic C₃A of cement is very low, while its sulphate content is high. This feature is important when conditioning the levels of adsorption of the admixtures [9].

3.2. Sodium montmorillonite clay (Na-MNT)

The clay used in this investigation is a powder sodium montmorillonite (Na-MNT) sample. Oxide composition by XRF is shown in Table 2 (expressed in wt. %). The BET-specific surface is measured at 49.5 m²/g (average of two measurements: 46.1 m²/g and 52.8 m²/g) and the average particle size (D₅₀), determined by laser diffraction, is 7.4 μm. A d₀₀₁ value of 12.3 Å is deduced from its 2θ position at 7.2° in XRPD analysis on raw (dry) clay powder. This value is typical for Na-MNT clays with one H₂O molecule layer inside the interlaminar space [10]. Some impurities are identified: 4.8 wt% of quartz and 3.3 wt% of calcite, which explains the loss-on-ignition (LOI) value. The cation exchange capacity (CEC) value reported in product specifications is 105 mmol/100 g, which agrees with the typical values for MNT clays [11].

3.3. Polycarboxylate-ether (PCE) polymers

Four different pure polycarboxylate-ether (PCE) polymers in aqueous solution are used (AA-1100, AA-2000, AA-3000 and AM-5800). The solid content and the structural characteristics of each PCE polymer are presented in Table 3. Complementary to the different PCE types, a superplasticizer based on calcium β-naftalensulfonate (Ca-BNS) is also used for comparison purposes. All admixtures are tested at an equal solid concentration of 20 wt%, prepared by dilution with distilled water.

3.4. Synthetic cement pore solution

All clay pastes are produced using synthetic cement pore solution as the liquid phase. The solution is prepared by dissolving 14.3 g of Na₂SO₄, 3.05 g of NaOH and 3.00 g of Ca(OH)₂ in 1 L of distilled freshly-boiled water (equivalent to 0.157 mol/l of OH⁻, 0.278 mol/l of Na⁺, 0.100 mol/l of SO₄²⁻ and 0.040 mol/l of Ca²⁺ concentration). The synthetic cement pore solution is always freshly prepared to avoid carbonation.

4. Experimental methods

4.1. Determination of PCE anionic charge

Anionic charge of PCE polymers is measured by the titration of free carboxylic groups with 0.5 M KOH solution freshly standardized with sulfamic acid. Mettler-Toledo DL28 equipment is used for the titration process. 10 g of 20 wt% PCE sample are diluted in 50 ml of distilled water and acidified with concentrated HCl, added drop by drop until a pH of 1.5 is reached. Titration with KOH is performed on the acidified samples until final pH value of 12–13 is reached. After the titration, two inflexion points are observed that correspond to the points of equivalence. The first point is attributed to the HCl surplus and the second point (located close to pH 9) is attributed to the neutralization of PCE carboxylic groups. The points of equivalence are identified using the method of incremental ratios [12]. The total PCE anionic charge is calculated using the difference in the KOH volume corresponding to the first and the

Table 3
Chemical structure and composition of PCE polymers.

Parameter	AA-1100	AA-2000	AA-3000	AM-5800
Solid concentration (wt. %)	50.3%	40.2%	35.9%	46.4%
Side chains	Type	IPEG	TPEG	VPEG
	mol EO/side chain	25	46	68
	Mw (g/mol)	1100	2000	3000
Main monomer of the backbone	Acrylic	Acrylic	Acrylic	Maleic

second inflexion points. The PCE anionic charge results are expressed as *mg KOH/g* or as *mol COOH/g PCE*.

4.2. Preparation of cement and clay pastes

Clay pastes are prepared at 22 °C by dispersing powdered Na-MNT clay in the synthetic cement pore solution at 17 wt% concentration. The mixing process is done using a vertical shaft mixer equipped with a helical head, moving at 600 rpm. The total mixing time is four minutes, during which the admixture is added at the required dosage after the one-minute mark. Cement pastes are prepared following the same procedure as clay pastes, using a water-to-cement (w/c) mass ratio of 0.26 and dispersing cement (and clay when used) with tap water at 22 °C. For cement pastes containing clay, both powders are dry-mixed prior to the addition of water.

4.3. Measurements of paste fluidity

Fluidity of cement and clay pastes is determined by the measurement of paste flow in the mini-slump test. The test uses a metallic truncated mini-cone that is 55 mm high, with an upper diameter of 19 mm and a lower diameter of 38 mm. The mini-cone is arranged on a flat, clean glass surface. It is filled with fresh paste and then compacted with a crystal rebar to evacuate trapped air. The mini-cone is then lifted to let the paste to flow onto the glass surface until the paste reaches maximum spread. The paste spread (paste flow, expressed in mm) is measured in two perpendicular directions and the average value is taken. This test is widely used to evaluate the fluidity of fresh cementitious pastes.

4.4. XRPD patterns of clay pastes

XRPD patterns for fresh and dried clay pastes are obtained following the experimental procedures previously described in [6]. In brief, *in-situ* XRPD analysis of fresh, unaltered clay pastes are performed using an MSPD diffractometer using synchrotron radiation at ALBA Synchrotron (Barcelona) and with a PANalytical X'Pert PRO MPD Cu K α lab diffractometer ($\lambda = 1.5418 \text{ \AA}$). The XRPD analysis of clay pastes centrifuged and then dried for seven days at 40 °C are performed with a Cu K α lab diffractometer.

4.5. Sorption of PCE polymers

The sorbed fraction of PCE polymers is measured by determination of the total organic carbon (TOC) with Shimadzu testing equipment. Freshly prepared cement pastes containing PCE polymers are diluted with Millipore water and mixed for 30 s. The suspension is

separated by centrifugation at 15,000 rpm for 10 min and the obtained liquid phase is filtrated with a 0.45 μm syringe Nylon filter. The final filtrate is acidified with concentrated HCl to remove inorganic carbon and is then submitted for TOC analysis by combustion at 900 °C. Same procedure is applied to measure PCE sorption in clay pastes prepared with synthetic cement pore solution.

Previously, calibration lines of each pure PCE polymer were prepared by recording the TOC value of three different concentrations of PCE [13]. The sorbed fraction of PCE is calculated by interpolation between the calibration lines from the difference of the total PCE dosage added and the non-sorbed fraction of PCE identified in the filtrate. Results are expressed as a percentage of sorption of the total PCE dosage and/or in sorbed mg of PCE per gram of cement or clay.

5. Results and discussion

5.1. Identification of PCE structural configuration

Table 4 shows the results of the PCE anionic charge obtained by titration. Considering an ideal structure in which the PCE backbone is exclusively composed of the main carboxylic monomer and knowing the molecular weight of the PEG/PEO side chains (reported in Table 3), the grafting ratio and the side chain frequency of each PCE is calculated from the measured anionic charge [14]. The calculated parameters are reported in Table 4.

The results presented in Table 3 indicate that the AA-2000 polymer is characterized by the highest grafting ratio, while AA-3000 possess the lowest content of side chains due to its highest anionic charge. At a comparable molecular weight, higher anionic charge values are attributed to a longer backbone length of the polymer [15]. Thus, AA-3000 and AA-1100 are polymers with presumably longer backbones than AA-2000 and AM-5800. AA-1100 and AM-5800 polymers present relevant differences in anionic charge, but their grafting ratios are similar. It is important to note that the AM-5800 polymers side chains are more than five times longer than the side chains of AA-1100, which means that there are significant differences in the structural configuration between both PCE polymers [16]. To account for the relationship between side chain length and side chain frequency, the parameter *side chain density* is defined as $[(\text{mol EO side chain}) \times (\text{side chain frequency})]$. The side chain density calculated for each PCE polymer is presented in Fig. 1.

The results shown in Fig. 1 indicates that AM-5800 is the PCE with the highest density of side chains due to the longest side chain length, despite not exhibiting the highest grafting ratio. AA-2000 is the PCE with the second highest side chain density

Table 4
Anionic charge and deducted side chain structure of studied PCE polymers.

Parameter		AA-1100	AA-2000	AA-3000	AM-5800
Anionic charge	mg KOH/g PCE	99	41	127	44
	mmol COOH/g PCE	1.77	0.73	2.27	0.79
Calculated side chain structure	Grafting ratio (mol side chain/mol carboxylic monomers)	1:2.2 (0.45)	1:1.5 (0.65)	1:8.1 (0.12)	1:2.4 (0.42)
	Side chain frequency (mol side chain/total mol in the backbone)	0.31	0.39	0.11	0.29

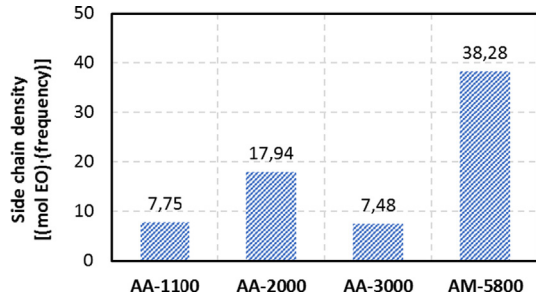


Fig. 1. Side chain density values calculated for PCE polymers.

due to its highest grafting ratio, despite a shorter side chain length than AA-3000. For AM-5800 and AA-2000 polymers, it is expected that important steric repulsion will be key in determining their adsorption behaviour [17]. AA-1100 and AA-3000 polymers present the lowest side chain densities, so steric effects will be lessened. However, due to their high anionic charge, they are expected to have a higher affinity for adsorption when compared to the AA-2000 and AM-5800 polymers [18].

5.2. Dispersion ability of PCE polymers in cement pastes with Na-MNT clay

The influence of the Na-MNT clay content on the fluidity of cement pastes is displayed in Fig. 2. Paste flow loss is evaluated with cement pastes containing 0.3% by cement weight (bcw) of PCE active solids and increasing quantities of Na-MNT clay (0%, 0.14%, 0.3%, 0.6% and 1.0% bcw) are added to verify its influence in the fluidity of cement pastes. Fig. 2(a) presents the average values of the initial flow of cement pastes at each percentage of clay, including the standard deviation for each individual measurement. For comparison purpose, the Ca-BNS polymer is also tested at 1.2% bcw dosage (in order to balance paste fluidity at a comparable level to PCE).

To provide a better comparison on the impact of clay dosage on the paste flow loss, Fig. 2(b) represents the *relative reduction of fluidity*, calculated by dividing the average paste flow loss at each clay dosage by the paste flow value of cement paste without Na-MNT clay. Therefore, a relative value of 1 corresponds to a total fluidity loss, while a relative value of 0 means no reduction of fluidity.

The specific capability of each PCE polymer to disperse cement particles can be determined from the initial paste flow values shown in Fig. 2(a) for cement paste samples without clay. AM-5800 has the highest cement dispersing capacity for the studied PCE polymers due to its longest side chains and highest side chain density [19]. AA-3000 shows similar performance to AM-5800 despite having shorter side chains and lower side chain density. This property can be attributed to AA-3000's high anionic charge, which promotes a larger quantity of polymer adsorbed on the cement particles, generating effective dispersion. This approach is supported by the hypothesis proposed by [20], in which the global dispersing ability of PCE polymers is defined simultaneously by the dispersing capacity of PCE (as consequence of its polymeric structure) and by the total amount of polymer adsorbed on cement. The AA-2000 PCE polymer shows lower capacity for cement dispersion than AM-5800 and AA-3000, despite its high side chain density, while AA-1100 is the PCE polymer that demonstrates the lowest paste flow value. The initial fluidity of cement paste with Ca-BNS is lower than that of AA-1100, even after being dosed up to four times more.

When Na-MNT clay is added to the cement pastes, all samples present a significant decrease in their fluidity, with the reduction being most obvious in PCE polymers. The significant reduction of PCE dispersion ability can be observed in Fig. 2(b) for all PCE polymers, even at the lowest clay dosage (up to 22% paste flow loss for AA-3000). Ca-BNS presents a totally different profile of paste flow loss. This observation is evidence that BNS condensates have much better tolerance to MNT clays than PCE polymers [18–21], and the described linear reduction of paste flow can be attributed simply to the increase of total water demand by the addition of clay.

The relative reduction of paste flow presented in Fig. 2(b) also confirms and highlights that the impact on the dispersing capacity of PCE polymers produced at equivalent Na-MNT dosages is not homogeneous for the different polymer structures used. AM-5800 and AA-3000 presents the maximum paste flow loss at all clay dosages, but demonstrate a more relevant impact at low clay contents. AA-2000 shows a similar impact at a low dosage of clay, but the interference on its dispersing ability at a higher clay dosage is comparatively lower than that of AM-5800 and AA-3000. The lowest relative reduction of paste flow observed in AA-1100 at all clay dosages suggests that this PCE structure has the most reduced clay sensitivity for all PCE polymers tested. Therefore,

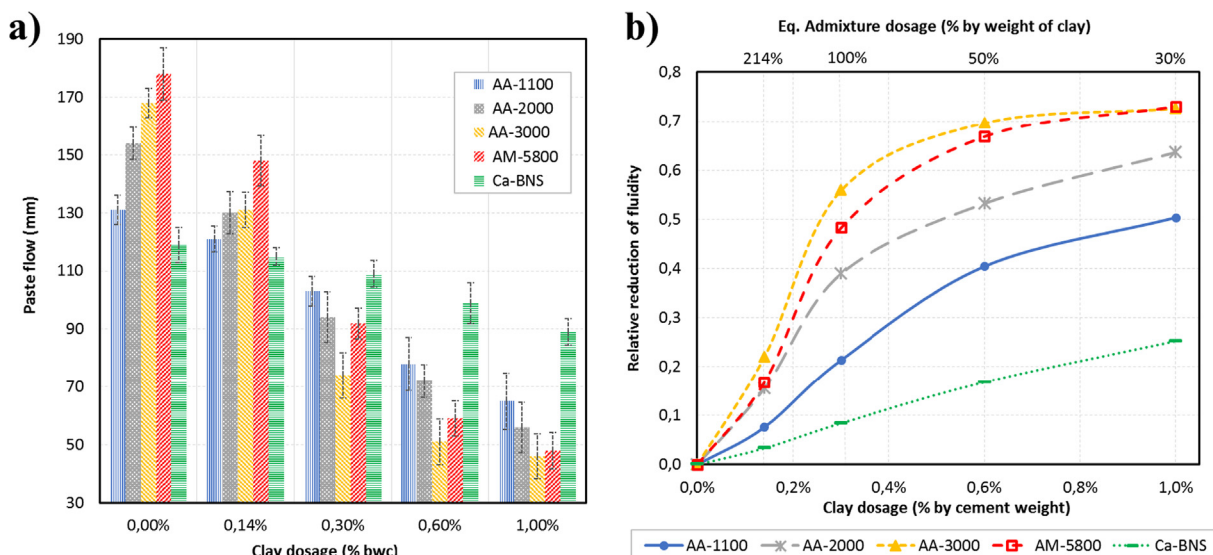


Fig. 2. a) Paste flow results of cement pastes with different amounts of Na-MNT clay, with standard deviation; b) Relative paste flow loss at each clay dosage.

according to the experimental paste flow results, it can be firmly stated that different PCE polymeric structures result in relevant differences on the paste flow loss of cement pastes containing Na-MNT clay.

5.3. Sorption rate of PCE polymers on cement pastes with Na-MNT clay

Fig. 3 presents the results of PCE sorption measurements performed just after completing the mixing process. The net sorbed amount of PCE measured on cement pastes without clay are presented in Fig. 3(a), including the percentage of sorbed PCE (on total PCE dosage). Fig. 3(b) shows the evolution of sorption rate measured in cement pastes including MNT clay at increasing dosages, expressed in the net amount of sorbed PCE (mg PCE/g) and in the sorption percentage on the total PCE weight.

The natural sorption behaviour of each PCE polymer on cement can be deduced from Fig. 3(a). AA-3000, followed by AA-1100, show the highest sorption rates, so they are the PCE polymers having the greatest affinity for the cement used. This is attributed to their high anionic charge, which promotes early adsorption on cement surface [17,22]. As expected, PCE polymers AA-2000 and AM-5800 show the lowest net sorption of polymer, in agreement with the lower anionic charge. Therefore, it indicates that the effective dispersion is produced by a lower amount of polymer than the AA-1100 and AA-3000 PCE polymer.

When Na-MNT clay is added to the cement pastes, both net sorption of PCE and the sorption percentage increase. Using Fig. 3(b), note that the progression of polymer sorption in cement pastes containing Na-MNT clay shows clear differences for the different PCE structures used and aligns with the paste flow results presented in Fig. 2. At a low dosage of clay, AA-3000 is the PCE type presenting the highest sorption rate, which slows down from 0.3% bwc of clay upwards. The AA-1100 polymer shows opposite behaviour when compared to that of AA-3000. AA-2000 and AM-5800 polymers present similar evolution of sorption rate, progressing between the levels of AA-1100 and AA-3000 up to a clay dosage level of 0.6% bwc. At this clay dosage, the sorption rate of AA-2000 and AM-5800 rises to AA-3000 values. At 1.0% clay dosage, AM-5800 shows the highest sorption within all the PCE polymers and AA-2000 and AA-1100 present similar values than that of AA-3000. In any case, at 1.0% bwc clay dosage all PCE polymers present comparable results of net sorption around 3.0 mg/g. It means that the sorbed fraction of PCE already reaches nearly 100%, as observed in Fig. 3(b). The level of sorbed fraction indicates that the PCE admixture is under clear stoichiometric limiting conditions, so that

there is not enough polymer to interact with all the sorption sites available in both the cement and clay colloids. Thus, any possible differences between sorption rates of each PCE structure cannot be identified from this clay dosage.

5.4. Expansion of Na-MNT by in-situ XRPD analysis on fresh clay pastes

In-situ XRPD analysis on fresh, unaltered clay pastes evaluates the evolution of the interlaminar space dimension (d_{001}) for Na-MNT clay produced by different dosages of PCE polymers. XRPD patterns are recorded at 0%, 2%, 5%, 13%, 50%, 100% and 220% dosage of PCE polymer by weight of clay. Table 5 displays the results of d-spacing (expressed in Å) corresponding to the main peaks identified by in-situ XRPD for each PCE polymer at each clay dosage tested (excluding equivalent peaks being second order reflections). Table 5 includes the results of d-spacing obtained by the traditional method of XRPD measurements. These results are displayed in Fig. 4(a) as a function of PCE dosage. Fig. 4(b) represents the d-spacing results obtained using the traditional testing methodology on centrifuged and dried clay pastes of equivalent composition.

Observed in Fig. 4(a) that the measured d-spacing evolution for fresh pastes progresses to much larger values in comparison to the results presented in Fig. 4(b), where XRPD measurements are performed on centrifuged and dried pastes. XRPD patterns obtained on dried clay pastes show maximum d-spacing value close to 21 Å for all PCE polymers tested, independent of their polymeric structure. These expansion rates are in agreement with results reported in other publications using the same experimental methodology [1–4]. In addition, there is no difference in d-spacing values for all PCE polymers upwards of the 50% dosage, where stationary state is reached.

The d-spacing variations measured using in-situ XRPD on fresh, unaltered clay pastes demonstrate a more complex absorption pattern (see Fig. 4(a)). Larger d-spacing values are recorded, indicating that a higher degree of side-chain intercalation is possible. It also indicates clear dependence on the PCE dosage [6]. Furthermore, one can observe that the evolution of clay expansion progresses differently for each PCE polymer, indicating that the polymeric structure has a more relevant role in the intercalation process than that previously suggested by the results reported by XRPD analysis on dried pastes. Therefore, in agreement with our previous publication [6], it can be stated that this methodology, in which diffraction data is taken in the clay powder obtained from centrifuged

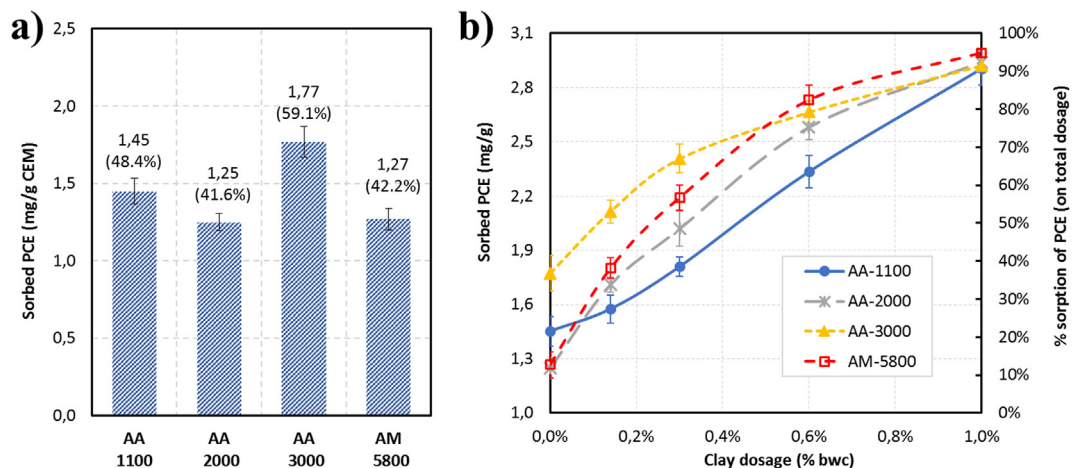
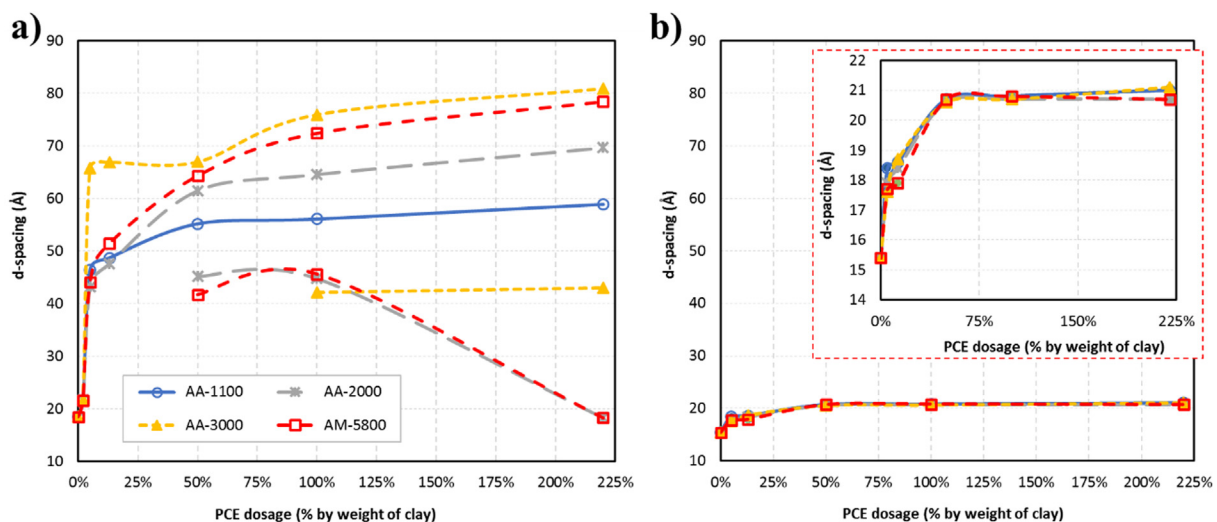


Fig. 3. Net sorbed amount of PCE and percentage of sorption (including standard deviation) of: a) Cement pastes without clay; b) Cement pastes including different amounts of Na-MNT clay.

Table 5Interlayer d-spacing (Å) from main peaks by *in situ* XRPD analysis; a) On fresh, unaltered clay pastes; b) On centrifuged and dried clay pastes.

Treatment method	PCE (wt% clay)	Main peaks	PCE type			
			AA-1100	AA-2000	AA-3000	AM-5800
Fresh, unaltered clay pastes	0	Peak 3	18.5			
	2	Peak 1	21.6	21.7	21.6	21.6
	5	Peak 1	46.4	43.2	65.8	44.1
	13	Peak 1	48.7	47.6	66.9	51.5
		Peak 3	–	18.3	18.3	18.3
	50	Peak 1	55.2	61.5	67.0	64.4
		Peak 2	–	44.8	–	41.7
		Peak 3	–	18.3	18.3	18.3
	100	Peak 1	56.1	64.6	76.0	72.5
		Peak 2	–	45.2	42.1	45.7
		Peak 3	–	18.3	18.3	18.3
		220	Peak 1	58.9	69.7	80.9
		Peak 2	–	–	43.0	–
		Peak 3	–	18.3	18.3	18.3
Centrifuged and dried clay pastes	0	Peak 1	15.4			
	5	Peak 1	18.4	17.9	17.6	17.7
	13	Peak 1	18.6	18.4	18.7	17.9
	50	Peak 1	20.7	20.6	20.6	20.7
	100	Peak 1	20.8	20.7	20.7	20.8
	220	Peak 1	21.0	20.7	21.1	20.7

**Fig. 4.** Expansion (d-spacing – d_{001} evolution) for Na-MNT clay from XRPD-SAXS patterns; a) On fresh clay pastes by *in-situ* XRPD; b) On centrifuged and dried clay pastes.

and dried PCE-treated clay pastes, likely giving incorrect results. This conclusion is in agreement with [23], which used molecular dynamics simulation of ethylene glycol intercalation in montmorillonite clay.

Fig. 4(a) describes a common model of d-spacing evolution for all the PCE polymers tested. The most significant changes in d-spacing are observed at a low dosage of PCE (from 2% to 13%). Despite describing all PCE types as a common profile of clay expansion, each polymeric structure shows a particular evolution of d-spacing. When the PCE dosage is higher than 50%, d-spacing variations tend to converge towards a nearly constant value, thus describing a stationary state. Each structure also demonstrates unique behaviour at the PCE dosage required to reach the stationary state and at the maximum d-spacing value produced at the stationary state.

The AA-3000 polymer shows the maximum clay expansion at low PCE dosage and its d-spacing at stationary state is the largest for all PCE polymers tested, 80 Å. AM-5800 shows a d-spacing value at stationary state similar than that of AA-3000, but it is

reached more progressively. The d-spacing evolution for AA-2000 at low PCE dosage progresses like AM-5800, but at a higher PCE dosage, it stabilizes earlier and on a lower value, 70 Å. AA-1100 is the polymer presenting the lowest d-spacing value, 60 Å, in the stationary state. Experimental results suggest that side chain length is controlling maximum d-spacing, so the higher expansion level affordable by the clay, which is larger for polymers with longer side chains. Nevertheless, no variation is observed between AA-3000 and AM-5800, presenting maximum d-spacings close to 80 Å. It is hypothesized that 80 Å is the maximum expansion that this clay can support to hold the integrity of the lamellar structure, making further expansion impossible.

Fig. 4(a) also reports the coexistence of various specimens with different degrees of side-chain intercalation, according the mechanism proposed by [6]. This phenomenon is only observed from 50% PCE dosage and higher and could be related to clay exfoliation. In any case, these specimens cannot be identified by XRPD analysis on dried clay pastes.

5.5. Exfoliation of Na-MNT induced by PCE polymers

Clay exfoliation is based on the progressive delamination of individual sheets forming the pristine clay particle and yields smaller clay particles with a reduced number of stacked plates [24]. The maximum level of exfoliation generates two-plates clay structures (the minimum configuration for clay nature) and even releases isolated plates [25]. For each layer delaminated from the primary clay particle, exfoliation produces a theoretical increase of the basal surface equivalent to double of the original. Therefore, due to the high ratio between the basal surface and edge surface that is typical of montmorillonite clays, exfoliation produces a huge increase in the total exposed clay surface available for adsorption [26–28].

When exfoliation occurs, one can hypothesize that it produces a reorganization of PCE units already absorbed into the interlaminal space. It looks coherent since the new active sites created on the new released basal surface of clay will demand further polymer for adsorption. Thus, PCE units already intercalated could be partially de-absorbed and migrate to occupy the vacant adsorption positions located in the new external basal surface created by exfoliation [28]. Therefore, clay exfoliation distorts the ratio between PCE content and the total reactive clay surface. In stoichiometry terms, the reactant PCE is moved towards limiting conditions. This statement is consistent with the simultaneous occurrence of new clay specimens having lower intercalation degree than that of the main unexfoliated main clay specimen. Moreover, exfoliation is a dynamic process of known kinetics, so it takes time to attain the equilibrium configuration [29].

For the specific Na-MNT clay used in this study, it is noted that from 80 Å, the structure of clay based on stacked plates is almost lost and, in parallel, exfoliation only begins if the interlayer d-spacing exceeds 60 Å. This behaviour suggests that the electrostatic forces stabilizing the layered structure become too weak between layers from beginning at 60 Å and they are almost largely ineffective upwards of 80 Å [30,31]. In between these two distances, delamination of the peripheral layers from the primary clay particle is produced and new, additional basal surface is released, according the schematic representation shown in Fig. 5.

The simultaneous coexistence of clay specimens with different interlayer d-spacing is observed for all the PCE polymers except AA-1100. It is the polymer having the shortest side chain length and its d-spacing at the stationary state is lower than 60 Å, making it the smallest of all polymers tested. Thus, it is assumed that no relevant clay exfoliation is produced for AA-1100 (regardless of the release of isolated clay plates). Clay pastes with AA-2000 and AM-5800 polymers present the earliest exfoliation signature at 50% dosage, due to the highest side chain density. For both polymers, new released clay specimens with d-spacing values of 40–45 Å can be observed simultaneously to the main clay specimen having a larger d-spacing. For 220% dosage of AA-2000 and AM-5800, clay specimens with 40–45 Å d-spacing are no longer observed and only a specimen with 18.3 Å d-spacing coexists with the main clay specimen. With the AA-3000 polymer, clay

exfoliation also produces new specimens with 42 Å interlayer d-spacing. Unlike AA-2000 and AM-5800, it is not observed until 100% dosage and it remains visible at 220% dosage, while the peak at 18.3 Å is not observed at any time. It is evident that the clay exfoliation induced by AA-3000 progresses differently than that of AA-2000 and AM-5800 polymers.

Thus, the study concludes that PCE polymers with higher side chain density promote clay exfoliation more quickly and extensively than polymers such as AA-3000 that have large side chains but reduced side chain density. Nevertheless, for AA-1100, no exfoliation signatures can be observed despite having a higher side chain density than AA-3000. This result suggests that side chains of 1100 g/mol are not large enough to induce clay exfoliation. One could also propose that clay exfoliation not only depends on side chain density, but also on side chain length.

To support the interpretation of clay exfoliation and its consequences, Kratky plots from the *in-situ* XRPD patterns of AM-5800 polymer are presented in Fig. 6(a). The diffraction patterns of AM-5800 obtained by *in-situ* XRPD analysis are presented in Fig. 6(b).

The representation of Kratky plots for Na-MNT clay with an increasing dosage of AM-5800 polymer allows for the identification of up to three peaks corresponding to clay specimens with different degrees of intercalation. Peak 1 corresponds to the main clay specimen with the largest d-spacing, associated to a higher number of intercalated side chains [6]. It can be observed that Peak 1 is not present when clay paste does not contain any PCE and it is visible only in pastes containing a PCE polymer. Peak 1 is present at every PCE dosage but is being displaced as the polymer dosage increases. Peak 2 refers to clay specimens with 42–46 Å interlayer d-spacing. This peak is not present in the clay pastes without a PCE polymer. Contrary to Peak 1, it is not fully recognized at the 13% PCE dosage. Peak 2 becomes visible at the AM-5800 dosages of 50% and 100% and demonstrates higher intensity at 100% than at 50%. At 220% dosage Peak 2 becomes negligible, meaning that the corresponding clay specimens with 42–46 Å d-spacing are nearly absent, likely due to additional exfoliations. Peak 3 at 18.5 Å is characteristic of Na-MNT clay in calcium alkaline solution in the absence of PCE polymers. This d-spacing size is associated to three water molecules absorbed in the interlayer region [10]. Peak 3, originally at 18.5 Å, remains always visible but it is being displaced to 18.3 Å when clay pastes include a PCE polymer. This d-spacing size is compatible with two layers of water molecules surrounding one layer of PEG/PEO side chain intercalated [32]. This means the minimum configuration possible for PCE intercalation since only one single side chain is absorbed. As seen in Fig. 6(a), the intensity of Peak 3 is similar at 13%, 50% and 100% dosage, but it increases at 220%. This behaviour suggests that at a 220% dosage of AM-5800, the clay specimen with the minimum configuration of side chains intercalation is present in relevant amounts. This is a result of thinner clay particles that are produced by multiple delamination of the Na-MNT clay, which leads the PCE polymer to limiting stoichiometric balance against the enlarged clay surface.

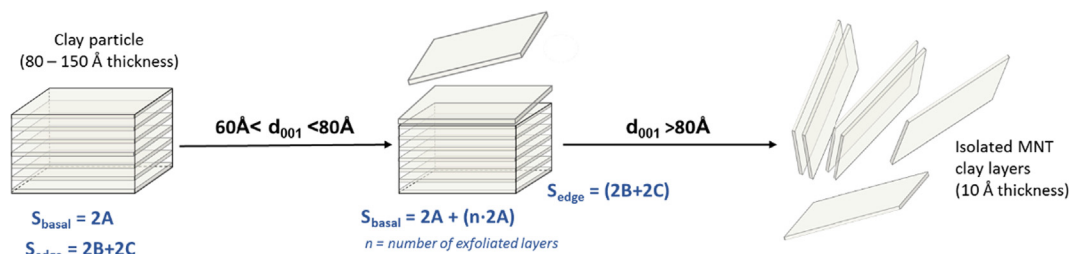


Fig. 5. Representation of MNT clay exfoliation and impact on the exposed, accessible basal and edge surface (adapted from [26]).

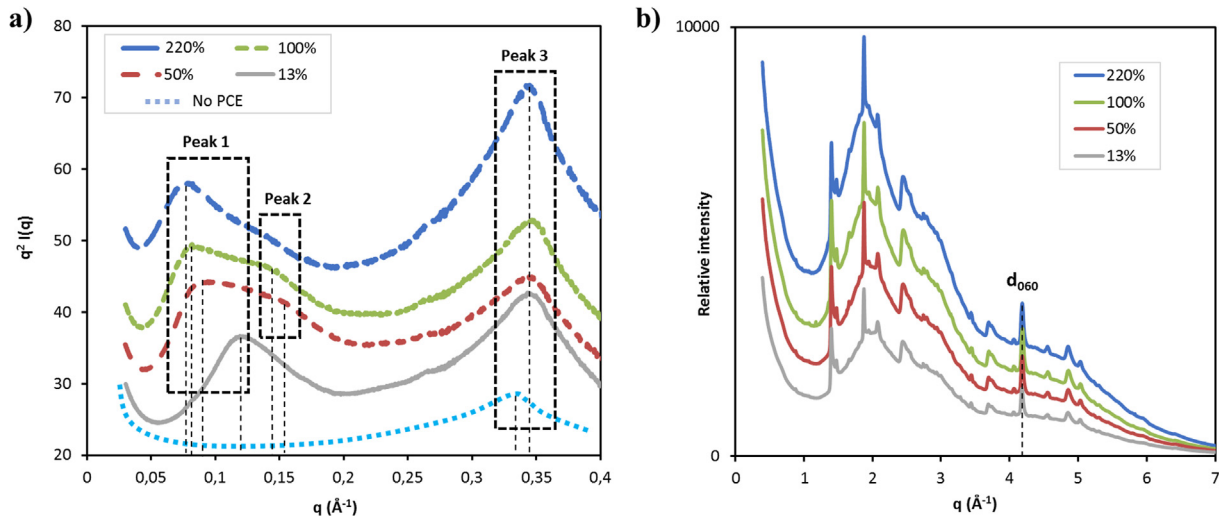


Fig. 6. a) Kratky plot for AM-5800 patterns; b) *in-situ* XRPD patterns of clay pastes with AM-5800 polymer.

One can observe that the shape of all peaks in the Kratky plots from Fig. 6(a) becomes broader at an increased PCE dosage. This characteristic is observed in all the PCE polymers tested and is attributed to the increased content of structural defects including turbostratic disorder by layer stacking [4]. This phenomenon is represented in Fig. 7.

Since the distance between clay plates enlarges when the PCE dosage is increased, it makes sense to suggest that turbostratic disorder increases when the interlaminal space is being expanded by the intercalation of PCE side chains. Under these conditions, clay exfoliation can be produced more easily [31]. Thus, it is hypothesized that the intercalation of PCE side chains has the capacity to promote exfoliation of montmorillonite clay and, as it is observed, this capacity increases in PCE polymers composed by large side chains and having high side chain density. An analogue behaviour is described in [34–38] by studying the effects of the length of linear PEO (poly-ethylene oxide) polymers for the synthesis of organo-clay nanocomposites from exfoliated clays, concluding that the longer the polymer chain, the higher the intercalation and the greater the exfoliation.

Observing the diffraction patterns presented in Fig. 6(b), the initial d_{060} peak, key to following the intralayer structure of MNT clays, does not change at any PCE dosage. This firmly indicates that the polymer intercalation in the interlaminal space is produced along the *c*-axis (layer stacking), while the intralayer structure, the *ab* plane, does not change [10]. It means that the structural alterations produced by PCE intercalation only affects the layer arrangement forming the clay colloid; meanwhile, the structure of the single clay plates remains unaltered [39].

5.6. Saturation dosage of Na-MNT clay by intercalation of PCE side chains

Observing the evolution of the interlayer *d*-spacing from Fig. 4 (a) at the low dosage range of PCE admixture (at low PCE/clay ratio, where PCE is the limiting reactant), it can be noticed that the PCE

polymers with the highest anionic charge (AA-3000 and AA-1100) produce a faster *d*-spacing increase. Thus, at low PCE/clay ratio, PCE polymers with a high anionic charge can intercalate larger number of side chain layers and reach the stationary state at lower PCE dosage, likely promoted by their higher adsorption affinity.

The saturation of the interlaminal space of the clay by PCE intercalation is described as the dosage of PCE needed to reach the stationary state (the state in which the *d*-spacing remains nearly static in response to additional PCE dosage). According to multiple intercalation mechanism proposed by [6], it is assumed to be the point at which the interlaminal space of MNT clay is saturated by intercalated PEO/PEG side chains, so almost no further units can be easily absorbed. Fig. 8(a) presents how the saturation dosage (D_{sat} , expressed as the percentage of PCE in the weight of clay) is calculated from the intersection point of the two lines, defined by the initial increase of *d*-spacing produced at a low dosage of PCE and the stationary state line. Fig. 8(b) displays the results of the saturation dosage - D_{sat} calculated for each studied PCE polymer.

Since the anionic charge defines the affinity of PCE polymers to interact with the clay surface, a relationship between D_{sat} -saturation dosage and the PCE anionic charge is expected. As seen in Fig. 8(c), the saturation dosage can be correlated with the PCE anionic charge. This relationship indicates that the saturation dosage decreases when the anionic charge of a PCE polymer increases but converges to a minimum residual value. The reported type of relationship between the saturation dosage and PCE anionic charge seems more likely than just a linear correlation as this would mean that PCE polymers with very high anionic charge would reach a saturation dosage equal to 0. That would imply that for practical purposes, there would be no intercalation.

5.7. Sorption isotherms of PCE polymers on Na-MNT clay

The results of the net sorbed amount of PCE measured in Na-MNT clay pastes containing increasing PCE dosages are presented

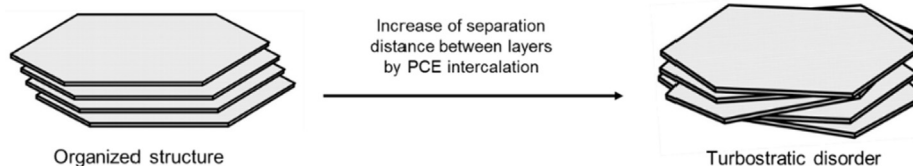


Fig. 7. Illustration of turbostratic disorder by layer stacking (adapted from [33]).

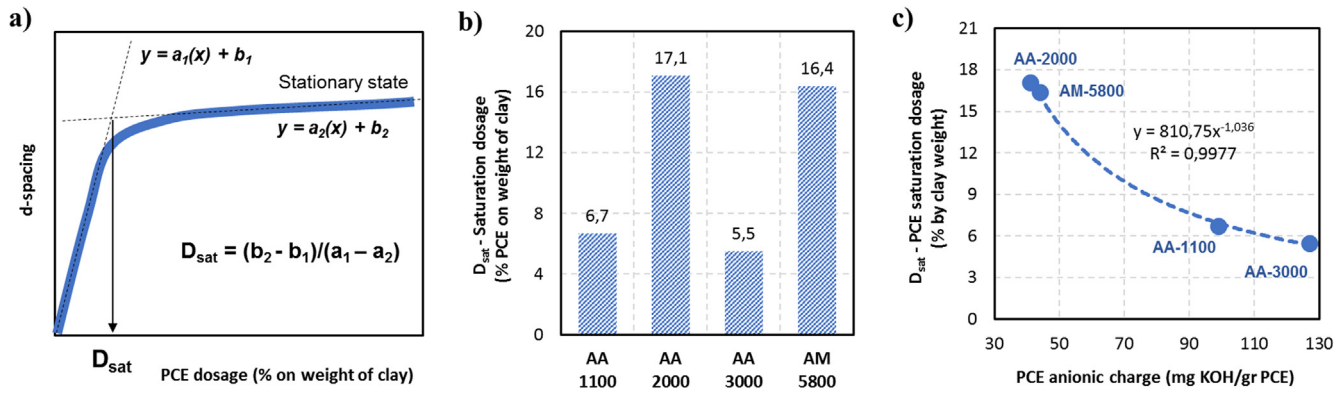


Fig. 8. a) Methodology for D_{sat} - saturation dosage calculation; b) D_{sat} - saturation dosage of each PCE; c) Correlation between saturation dosage and PCE anionic charge.

in Table 6. To identify the relative variations in the sorption rate at each PCE dosage, Fig. 9(a,b) displays the relative incremental of sorbed PCE (S_{rel}). It is calculated using the expression $\Delta S(x)_{rel} = (S_x - S_y)/(D_x - D_y)$, where $\Delta S(x)_{rel}$ means the relative incremental of sorption at a PCE dosage of D_x (expressed as mg PCE/g clay), S_x is the sorbed amount at the D_x dosage and S_y is the sorbed amount at the previous PCE dosage (D_y).

Interestingly, the relative incremental of sorbed PCE presented in Fig. 9 is consistent with both the expansion profile of the clay and the exfoliation behaviour deduced from the XRPD patterns. At a low PCE/clay dosage ratio (Fig. 9(a)), the PCE polymers with a higher anionic charge (AA-1100 and AA-3000) experience the greatest incremental of sorption, showing ΔS_{rel} values close to 1. It means that nearly 100% of the added polymer is being sorbed by the clay. It is the expected trend because the affinity for adsorption is driven by the PCE anionic charge. Conversely, when PCE/clay dosage ratio increases, Fig. 9(b) demonstrates that the greatest relative incremental of sorption is experienced by the AA-2000 and AA-5800 polymers. These are the PCE polymers with the highest side chain density, thus the polymers that are expected to promote the greatest clay exfoliation. Therefore, the trend observed in the sorption rates supports the proposed interpretation in regards of the consequences of the new, additional basal clay surface released by exfoliation.

5.8. Intercalation degree of PCE side chains

The number of PEO/PEG side chain units intercalated into Na-MNT clay can be calculated from the d-spacing results following the methodology proposed in [6]. Fig. 10 presents the intercalation degrees (n_{PEG}) obtained for PCE polymers at each tested dosage, including the main clay specimen and the clay specimens likely originated by exfoliation.

It is interesting to see that there are some preferred degrees of intercalation present in almost all PCE polymers. For the clay sample used, these preferred degrees are $n_{PEG} = 6-7$ and $n_{PEG} = 9-10$. Conversely, intercalation degrees corresponding to 3, 4 and 5 units

of PEO/PEG side chains are not observed in any case. This behaviour suggests that some intercalation degrees are more stable than others and they are presumably defined by the properties of the clay and not by the PCE polymer.

For all the new clay specimens produced by exfoliation, two intercalation degrees are only identified. The first observed specimen from exfoliation always presents six units of intercalated side chains ($n_{PEG} = 6$). This intercalation degree is visible for all the PCE polymers that are able to produce clay exfoliation (AA-2000, AA-3000 and AM-5800) but it is also commonly observed in the main, unexfoliated clay specimens, which suggests that it is a very stable configuration. Further exfoliation generates clay specimens with only one single intercalated side-chain layer ($n_{PEG} = 1$, at 18.3 Å d-spacing), which corresponds to the minimum possible configuration of intercalation. The intercalation degree $n_{PEG} = 1$ is exclusively observed in PCE polymers with high side chain density like AA-2000 and AM-5800 and it is not present in AA-3000, which only produces exfoliated specimens with $n_{PEG} = 6$ (six intercalated side-chain layers).

Using Fig. 10, it is also observed that a 2% dosage of any of the PCE polymers always produce the same intercalation degree of $n_{PEG} = 2$, with two units of side chains intercalated. Therefore, considering that the Na-MNT clay dispersed in calcium alkaline media presents an interlayer d-spacing equivalent to three water molecule layers absorbed into the interlaminar space [10] and, in parallel, the intercalation degree produced at the lowest PCE dosage always corresponds to two units of side chains ($n_{PEG} = 2$), it suggests that the mechanism of side chain intercalation is not based on the replacement of the absorbed water layers, but by the insertion of the PEO/PEG side chains in between the water layers that are already absorbed.

6. Interpretation of the intercalation mechanism of PCE side chains

It has been observed that the anionic charge of PCE is the main driver force defining the PCE dosage to saturate the interlaminar

Table 6 Net sorbed amount of PCE in clay pastes with increasing PCE dosages, including the standard deviation of the experimental results.

PCE dosage (% by weight of clay)	Net sorbed amount of PCE on clay (mg/g)			
	AA-1100	AA-2000	AA-3000	AM-5800
0%	0	0	0	0
2%	19 ± 3	17 ± 2	20 ± 1	18 ± 3
5%	48 ± 6	36 ± 4	50 ± 2	43 ± 5
13%	90 ± 8	68 ± 6	107 ± 9	75 ± 3
50%	163 ± 13	143 ± 10	181 ± 6	188 ± 14
100%	204 ± 9	226 ± 15	228 ± 12	243 ± 11
150%	216 ± 12	259 ± 13	243 ± 16	290 ± 19
220%	218 ± 11	277 ± 13	263 ± 17	308 ± 21

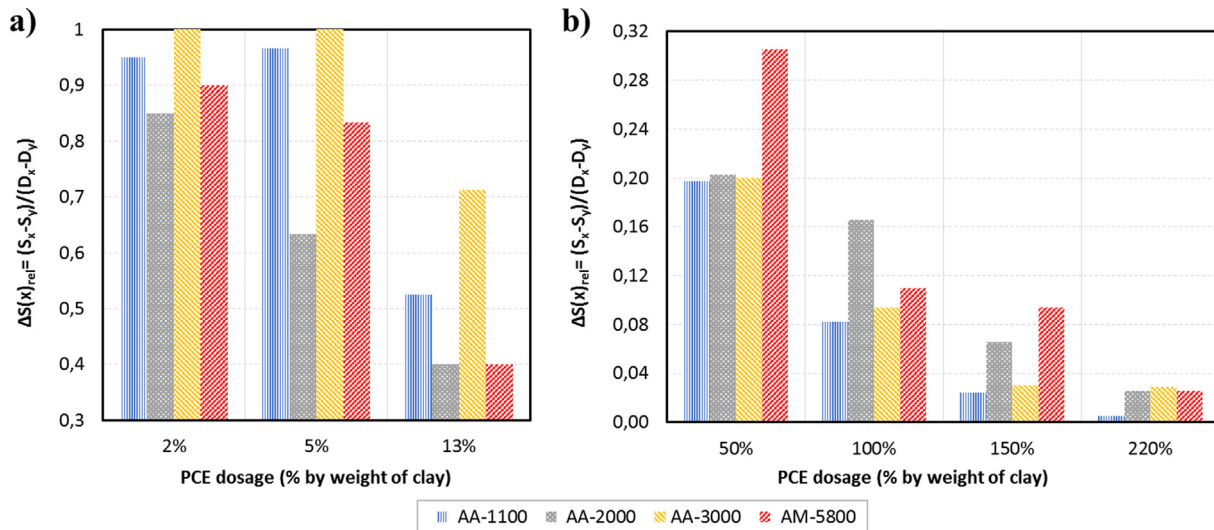


Fig. 9. Relative incremental of sorption (ΔS_{rel}) at each PCE dosage; a) From 2% to 13% PCE dosage; b) From 50% to 220% PCE dosage.

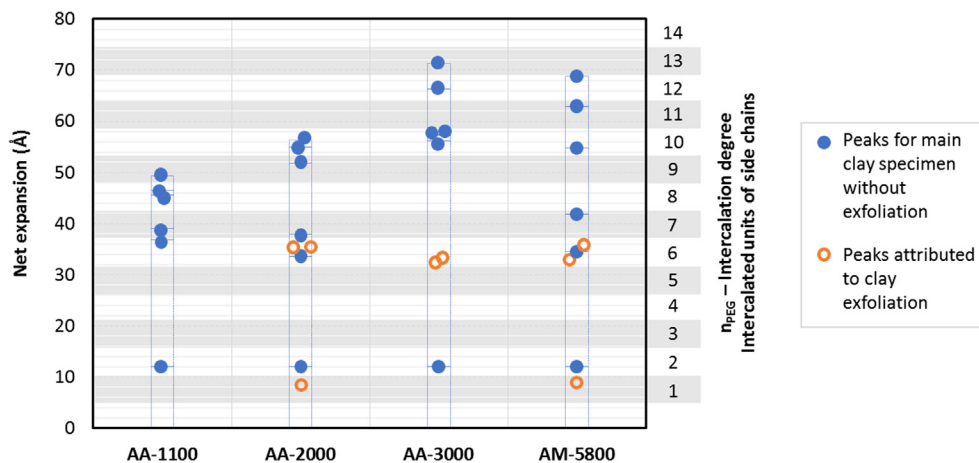


Fig. 10. Intercalation degrees (n_{PEG}) of PCE side chains into Na-MNT clay.

space of the clay. PCE polymers with higher anionic charge promote the adsorption of polymer on the clay surface, allowing it to reach the saturation dosage sooner. In parallel, PCE polymers with longer side chain length and especially those with higher side chain density have an increased tendency to produce clay exfoliation. Therefore, for these polymeric structures, a greater fluidity loss and a higher level of sorption is expected due to the generation of new basal surface area produced when clay exfoliates. In this way, the results of relative reduction of paste flow presented in Fig. 2(b) and the relative incremental of sorption presented in Fig. 9(b) for AA-2000 and AA-5800 polymers match with this hypothesis, since these are the polymers with the highest side chain density. Conversely, the AA-1100 polymer, having reduced side chain density and the shortest side chains, shows the lowest degree of intercalation. This behaviour aligns with the lowest reduction of paste flow observed in Fig. 2(b) and with the lowest sorption rate at high dosage of AA-1100, in Fig. 9(b). Nevertheless, the AA-3000 polymer, having lower side chain density than AA-1100, demonstrates a fluidity loss profile more similar to AM-5800 than that of the AA-1100. This behaviour of the AA-3000 polymer can be attributed to its side chain length (which falls in between those of polymers AA-2000 and AM-5800). Consequently, it can be proposed that the clay exfoliation induced by the interca-

lation of PCE polymers depends on the concentration of side chains in the edge opening between clay plates (being higher in the case of high side chain density) and on the capacity of the side chains to penetrate into the interlamellar space (being deeper in the case of large side chains [40]). This interpretation is consistent with the relative incremental of sorption presented in Fig. 9(b) for the AA-300 polymer.

Based on this reasoned hypothesis, a model for the intercalation behaviour of PCE side chains into Na-MNT clay is presented in Fig. 11 considering the adsorption location of the polymer. Since MNT clays that are dispersed in alkaline cement pore solution cumulates anionic charges in both the edge surface (by the ionization of the silanol, aluminate pH dependant terminals) and the basal surface (by the ionization of soluble cations balancing the permanent charges induced by octahedral substitution) [41–44], it is assumed that PCE polymers can be adsorbed on both clay locations.

PCE units adsorbed on the edge surface -case (a) in Fig. 11- will be easily intercalated, since the distance to the interlayer openings is reduced and accessible, even for PCE having short side chains. The side chains of PCE units adsorbed in the basal surface of Na-MNT clay also can be intercalated if the location of adsorption is near the edge area -case (b) in Fig. 10-, since the rotation of -C-

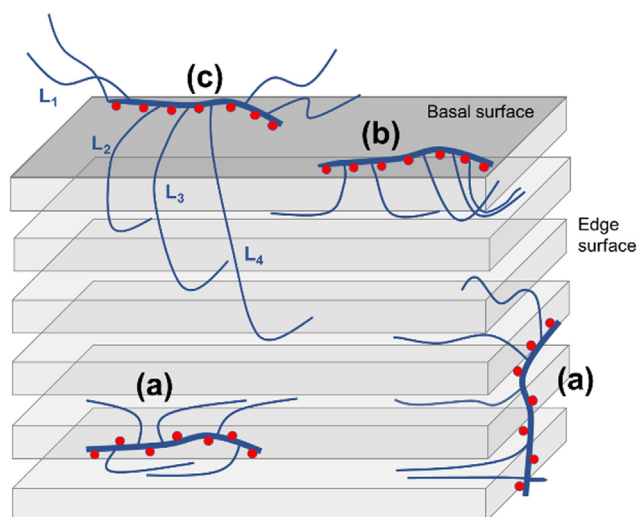


Fig. 11. Intercalation models of side chains of PCE polymers depending on the adsorption location of the PCE on the Na-MNT clay surfaces (not at scale).

O-C bonds allows the side chains to be displayed optimally for intercalation. When the PCE units are adsorbed in the central locations of the basal surface -case (c)-, intercalation will only be possible if PCE side chains are long enough to rotate and reach the interlayer openings. Since the typical thickness/width ratio for montmorillonite clay is up to 1/200 [45], most PCE units adsorbed on the basal planes will be located too far to intercalate their side chains, except for PCE polymers with very long side chains. This hypothesis justifies the behaviour of the AA-3000 polymer, which shows the largest d-spacing at the stationary state with similar value to AM-5800. The same argument is valid for AA-1100, which presents the lowest d-spacing, since the accessibility to the interlaminar spaces is restricted by its short side chains. The stationary d-spacing for AA-2000 is larger than AA-1100, but lower than both AA-3000 and AM-5800, despite having the highest side chain density. Once again, the same interpretation fits because AA-2000 contains shorter side chains than AA-3000 and AM-5800 but longer than AA-1100, thus limiting the intercalation of PCE units adsorbed on the basal surface of the clay but in a lesser extent than for AA-1100.

7. Conclusions

Using *In-situ* XRPD analysis on fresh, unaltered MNT pastes containing PCE-based superplasticizers, a new scenario for the intercalation behaviour of PCE side chains is revealed. The influence of the polymeric structure of the PCE on the intercalation behaviour can be distinguished from the d-spacing results and the experimental data of clay expansion allows for the establishment of a logic relationship with the results of paste flow loss and sorption behaviour.

Contrary to conclusions drawn from XRPD analysis performed on dried clay pastes, *in-situ* XRPD analysis on fresh, unaltered clay pastes confirms that the polymeric structure of PCE-based superplasticizers has a key role in the progression of the side chain intercalation and the evolution of the interlayer d-spacing, while meeting alignment with the experimental results of paste flow and sorption rate. The major parameters of the structure of PCE polymers influencing on the intercalation behaviour into Na-MNT clay are identified below:

- When the PCE/clay ratio is high, clay exfoliation is produced, generating additional exposed, accessible clay surface. It forces a reorganization of PCE arrangement around the clay colloid. As

consequence of clay exfoliation, there is an amplified impact on the fluidity loss. Experimental results of paste flow loss in cement pastes at low clay dosage support this scenario.

- PCE polymers with high side chain density produces earlier and more severe exfoliation, leading to an increase of fluidity loss even at a very high PCE/clay ratio (in which a very low amount of clay is present in the cement pastes).
- Maximum d-spacing (stationary d-spacing) is produced at the stationary state, when the PCE/clay ratio is highest. Stationary d-spacing is larger for PCE polymers having long side chains but is restricted by the stability of the clay structure (which exfoliates from a certain d-spacing value).
- When the PCE/clay ratio is low, d-spacing progression is controlled by the adsorption capacity, thus, by the anionic charge of the PCE polymer. Polymers with a higher anionic charge saturate the interlaminar space of the clay at a lower PCE/clay ratio.

Consequently, examining the d-spacing perspective, a consistent explanation has been found to justify that the PCE polymers with large side chains and high side chain density present higher sensitivity to MNT clays than PCE structures with shorter side chains and reduced side chain density. It matches with the behaviour observed with the AA-1100 polymer, which is the PCE with the lowest sensitivity to MNT clay within all polymers used.

Additionally, a new model is presented that explains the relationship between the structure of PCE polymers and the intercalation mechanism of side chains into MNT clays. This model is endorsed by the consistency between experimental results of paste flow and sorption rate and the d-spacing values obtained by *in-situ* XRPD measurements.

To complement this investigation and its corresponding conclusions, additional research is suggested to identify the influence of the PCE molecular weight in the intercalation behaviour. In addition, the potential influence of Na-MNT properties in the d-spacing evolution has not been investigated (either the octahedral substitution rate or shape and size of clay particles). Finally, the potential impact of mixing speed and shear energy and their influence on clay exfoliation and side chains intercalation degree is a topic for investigation.

Declaration of Competing Interest

None.

Acknowledgments

Mr. Borralleras thanks all the support given by BASF Construction Chemicals to the development of this work. Dr. I. Segura is supported by the postdoctoral Torres Quevedo program of the Spanish Ministry of Economy and Competitiveness.

References

- [1] L. Lei, J. Plank, Synthesis and properties of a vinyl ether-based polycarboxylate superplasticizer for concrete possessing clay tolerance, *Ind. Eng. Chem. Res.* 53 (2014) 1048–1055, <https://doi.org/10.1021/ie4035913>.
- [2] H. Tan, Xin Li, M. Liu, B. Ma, B. Gu, X. Li, Tolerance of cement for clay minerals: effect of side-chain density in polyethylene oxide (PEO) superplasticizers additives, *Clay Clay Minerals* 64–6 (2016) 732–742, <https://doi.org/10.1346/CCMN.2016.064050>.
- [3] H. Tan, B. Gu, B. Ma, X. Li, C. Lin, Mechanism of intercalation of polycarboxylate superplasticizer into montmorillonite, *Appl. Clay Sci.* 129 (2016) 40–46, <https://doi.org/10.1016/j.clay.2016.04.020>.
- [4] S. Ng, J. Plank, Interaction mechanisms between Na-montmorillonite clay and MPEG-based polycarboxylate superplasticizers, *Cem. Concr. Res.* 42 (2012) 847–854, <https://doi.org/10.1016/j.cemconres.2012.03.005>.
- [5] G. Xing, W. Wang, G. Fang, Cement dispersion performance of superplasticizers in the presence of clay and interaction between superplasticizers and clay,

- Adv. Cem. Res. 29 (2017) 194–205, <https://doi.org/10.1016/j.arabjc.2017.12.027>.
- [6] P. Borralleras, I. Segura, M.A.G. Aranda, A. Aguado, Influence of experimental procedure on d-spacing measurement by XRD of montmorillonite clay pastes containing PCE based superplasticizer, *Cem. Concr. Res.* 116 (2019) 266–272, <https://doi.org/10.1016/j.cemconres.2018.11.015>.
- [7] S. Qian, H. Jiang, B. Ding, Y. Wang, C. Zheng, Z. Guo, Synthesis and performance of polycarboxylate superplasticizer with clay-inerting and high slump retention capability, *Mater. Sci. Eng.* 182 (2017), <https://doi.org/10.1088/1757-899X/182/1/012033>.
- [8] D. Atarashi, K. Yamada, A. Ito, M. Miyauchi, E. Sakai, Interaction between montmorillonite and chemical admixture, *J. Adv. Concr. Technol.* 13 (2015) 325–331, <https://doi.org/10.3151/jact.13.325>.
- [9] R. Magarotto, I. Torresan, N. Zeminian, Effect of alkaline sulphates on the performance of superplasticizers, in: 11th International Congress on the Chemistry of Cement, 2003, pp. 569–579.
- [10] M. Matuszewicz, K. Pirkkalainen, J.P. Suuronen, A. Root, A. Muurinen, R. Serimaa, M. Olin, Microstructural investigation of calcium montmorillonite, *Clay Miner.* 48 (2013) 267–276, <https://doi.org/10.1180/claymin.2013.048.2.08>.
- [11] D.L. Rowell, *Soil Science: Methods and Applications*, Longman Scientific and Technical Publications, 1993, p. 133. ISBN 0-470-22141-0.
- [12] A. Checchetti, J. Lanzo, Qualitative measurement of pH and mathematical methods for the determination of the equivalence point in volumetric analysis, *World J. Chem. Educ.* 3 (2015) 64–69, <https://doi.org/10.12691/wjce-3-3-2>.
- [13] H. Tan, B. Gu, Y. Guo, B. Ma, J. Huang, J. Ren, F. Zou, Improvement in compatibility of polycarboxylate superplasticizers with poor-quality aggregate containing montmorillonite by incorporating polymeric ferric sulfate, *Constr. Build. Mater.* 162 (2018) 566–575, <https://doi.org/10.1016/j.conbuildmat.2017.11.166>.
- [14] J. Plank, B. Sachsenhauser, Experimental determination of the effective anionic charge density of polycarboxylate superplasticizers in cement pore solution, *Cem. Concr. Res.* 39 (2009) 1–5, <https://doi.org/10.1016/j.cemconres.2008.09.001>.
- [15] D. Wilinski, P. Lukowski, G. Rokicki, Polymeric superplasticizers based on polycarboxylates for ready-mixed concrete: current state of the art, *Polimery* 61 (2016) 474–481, <https://doi.org/10.14314/polimery.2016.474>.
- [16] R.J. Flatt, I. Schober, E. Raphael, C. Plassard, E. Lesniewska, Conformation of adsorbed comb copolymers dispersants, *Langmuir* 25 (2009) 845–855, <https://doi.org/10.1021/la801410e>.
- [17] X. Shu, Q. Ran, J. Liu, H. Zhao, Q. Zhang, X. Wang, Y. Yang, Tailoring the solution conformation of polycarboxylate superplasticizer toward the improvement of dispersing performance in cement paste, *Constr. Build. Mater.* 116 (2016) 289–298, <https://doi.org/10.1016/j.conbuildmat.2016.04.127>.
- [18] G. Xing, W. Wang, J. Xu, Grafting tertiary amine groups into the molecular structures of polycarboxylate superplasticizers lowers their clay sensitivity, *RSC Adv.* 6 (2016) 106921–106927, <https://doi.org/10.1039/C6RA22027D>.
- [19] C. Zhi Li, N. Feng, Y. De Li, R. Chen, Effects of polyethylene oxide chains on the performance of polycarboxylate-type water-reducers, *Cem. Concr. Res.* 25 (2005) 867–873, <https://doi.org/10.1016/j.cemconres.2004.04.031>.
- [20] J. Liu, Q. Ran, C. Miao, M. Qiao, Effects of grafting densities of comb-like copolymer on the dispersion properties of concentrated cement suspensions, *Mater. Trans.* 53 (2012) 553–558, <https://doi.org/10.2320/matertrans.M2011344>.
- [21] L. Lei, J. Plank, A study on the impact of different clay minerals on the dispersing force of conventional and modified vinyl ether based polycarboxylate superplasticizers, *Cem. Concr. Res.* 60 (2014) 1–10, <https://doi.org/10.1016/j.cemconres.2014.02.009>.
- [22] C. Giraudeau, J. dEspinose de Lacaillerie, Z. Souguir, Surface and intercalation chemistry of polycarboxylate copolymers in cementitious systems, *J. Am. Ceram. Soc.* 92 (2009) 2471–2488, <https://doi.org/10.1111/j.1551-2916.2009.03413.x>.
- [23] M. Szczerba, Z. Klapyta, A. Kalinichev, Ethylene glycol intercalation in smectites Molecular dynamics simulation studies, *Appl. Clay Sci.* 91 (2014) 87–97, <https://doi.org/10.1016/j.clay.2014.02.014>.
- [24] H. Li, Y. Zhao, S. Song, Y. Hu, Y. Nahmad, Delamination of Na-montmorillonite particles in aqueous solutions and isopropanol under shear forces, *J. Dispersion Sci. Technol.* 38 (2017) 1117–1123, <https://doi.org/10.1080/01932691.2016.1224720>.
- [25] X. Zhang, H. Yi, H. Bai, Y. Zhao, F. Min, S. Song, Correlation of montmorillonite exfoliation with interlayer cations in the preparation of two-dimensional nanosheets, *RSC Adv.* 7 (2017) 41471–41478, <https://doi.org/10.1039/C7RA07816A>.
- [26] J. Torres-Lunam, J.G. Carriazo, N.R. Sanabria, Arcillas delaminadas por especies de titanio – degradación de un colorante textil (amarillo reactivo 145), in: *Proceedings XXIV Congreso Iberoamericano de Catálisis*, 2014, pp. 112–119.
- [27] E.C. Jonas, R.M. Oliver, Size and shape of montmorillonite crystallites, *Clay Clay Miner.* 15 (1967) 27–33, <https://doi.org/10.1346/CCMN.1967.0150103>.
- [28] N. Güven, Smectites – hydrous phyllosilicates, *Rev. Mineral.* 19 (1988) 497–560.
- [29] S.W. Kim, W.H. Jo, M.S. Lee, M.B. Ko, J.Y. Jho, Effects of shear on melt exfoliation of clay in preparation of Nylon 6/organoclay nanocomposites, *Polym. J.* 34 (2002) 103–111, <https://doi.org/10.1295/polymj.34.103>.
- [30] T. Chen, Y. Yuan, Y. Zhao, F. Rao, S. Song, Effect of layer charges on exfoliation of montmorillonite in aqueous solutions, *Colloids Surfaces: Physicochem. Eng. Aspects* 548 (2018) 92–95, <https://doi.org/10.1016/j.colsurfa.2018.03.066>.
- [31] R.F. Geise, The electrostatic interlayer forces of layer structure minerals, *Clay Clay Miner.* 26 (1978) 51–57, <https://doi.org/10.1346/CCMN.1978.0260106>.
- [32] R. Ait-Akbour, P. Boustingorry, F. Leroux, F. Leising, C. Taviot-Guého, Adsorption of polycarboxylate poly(ethylene glycol) (PCP) esters on montmorillonite (MNT): Effect of exchangeable cations (Na⁺, Mg²⁺ and Ca²⁺) and PCP molecular structure, *J. Colloids Interface Sci.* 437 (2015) 227–234, <https://doi.org/10.1016/j.jcis.2014.09.027>.
- [33] A. Meunier, Why are clay minerals small?, *Clay Miner* 41 (2006) 551–566, <https://doi.org/10.1180/0009855064120205>.
- [34] S. Zhu, H. Peng, J. Chen, H. Li, Y. Cao, Y. Yang, Z. Feng, Intercalation behaviour of poly(ethylene glycol) in organically modified montmorillonite, *Appl. Surf. Sci.* 276 (2013) 502–511, <https://doi.org/10.1016/j.apsusc.2013.03.123>.
- [35] A. Kobayashi, M. Kawaguchi, T. Kato, A. Takahashi, Intercalation adsorption of poly(ethylene oxide) into montmorillonite, *Kyoto Univ. – Bull. Inst. Chem. Res.* 66 (1989) 176–183.
- [36] M. Reinholdt, R. Kirkpatrick, T. Pinnavaia, Montmorillonite-poly(ethylene glycol) nanocomposites: interlayer alkali metal behaviour, *J. Phys. Chem.* 109 (2005) 16296–16303, <https://doi.org/10.1021/jp052601o>.
- [37] T. Okada, Y. Seki, M. Ogawa, Designed nanostructures of clay for controlled adsorption of organic compounds, *J. Nanosci. Nanotechnol.* 14 (2014) 2121–2134, <https://doi.org/10.1166/jnn.2014.8597>.
- [38] R.W. Franco, C. Brasil, G. Mantovani, E. de Azevedo, T. Bonagamba, Molecular dynamics of poly(ethylene glycol) intercalated in clay, studied using ¹³C solid-state NMR, *Materials* 6 (2013) 47–64, <https://doi.org/10.3390/ma6010047>.
- [39] R. Tettenhorst, H.E. Roberson, X-ray diffraction aspects of montmorillonite, *Am. Mineral.* 58 (1973) 73–80.
- [40] H. Li, Y. Zhao, T. Chen, Y. Nahmad, S. Song, Restraining Na-montmorillonite delamination in water by adsorption of sodium dodecyl sulfate or octadecyl trimethyl ammonium chloride on the edges, *Minerals* 6 (2016) 87–97, <https://doi.org/10.3390/min6030087>.
- [41] T. Preocanin, A. Abdelmonem, G. Montavon, J. Luetzenkirchen, Charging behaviour of clays and clay minerals in aqueous electrolyte solutions. Experimental methods for measuring the charge and interpreting the results – Clays, clay minerals and ceramic materials based on clay minerals, ISBN 978-953-51-2259-3 (2016). <https://doi.org/10.5772/62082>
- [42] X. Liu, X. Lu, M. Sprik, J. Cheng, E.J. Meijer, R. Wang, Acidity of edge surface sites of montmorillonite and kaolinite, *Geochim. Cosmochim. Acta* 117 (2013) 180–190, <https://doi.org/10.1016/j.gca.2013.04.008>.
- [43] M. Alvarez-Silva, M. Mirnezami, A. Uribe-Salas, J.A. Finch, Point of zero charge, isoelectric point and aggregation of phyllosilicate minerals, *Canada Metall. Q.* 49 (2010) 405–410, <https://doi.org/10.1179/cmjq.2010.49.4.405>.
- [44] E. Tombácz, M. Szekeres, Colloidal behaviour of aqueous montmorillonite suspensions: the specific role of pH in the presence of indifferent electrolytes, *Appl. Clay Sci.* 27 (2004) 75–94, <https://doi.org/10.1016/j.clay.2004.01.001>.
- [45] R. Holtz, W. Kovacs, *An Introduction to Geotechnical Engineering*, Prentice-Hall Inc., 1981. ISBN 013-484394-0.